HHS Public Access

Author manuscript

Nat Med. Author manuscript; available in PMC 2012 June 01.

Published in final edited form as:

Nat Med. ; 17(12): 1594–1601. doi:10.1038/nm.2542.

Mesenchymal Stem Cell-Based Tissue Regeneration is Governed by Recipient T Lymphocyte *via* IFN-γ and TNF-α

Yi Liu[1,2], **Lei Wang**[1,3], **Takashi Kikuiri**[1], **Kentaro Akiyama**[1], **Chider Chen**[1], **Xingtian Xu**[1,4], **Ruili Yang**[1], **WanJun Chen**[5], **Songlin Wang**[2], and **Songtao Shi**[1,*]

[1]Center for Craniofacial Molecular Biology, Ostrow School of Dentistry, University of Southern California, 2250 Alcazar Street, CSA 103, Los Angeles, CA 90033, USA University of Southern California, 2250 Alcazar Street, CSA 103, Los Angeles, CA 90033, USA

[2]Molecular Laboratory for Gene Therapy and Tooth Regeneration, Capital Medical University School of Stomatology, Tian Tan Xi Li No. 4, Beijing 100050, China

[3]Fourth Military Medical University School of Stomatology, Xi'an, Shanxi 710032, China

[4]Key Laboratory of Translational Research, Tong Ji University School of Stomatology, No. 399 Yan Chang Zhong Road, Shanghai 200072, China

[5]National Institute of Dental and Craniofacial Research, National Institutes of Health, Bethesda, Maryland, USA

Abstract

Stem cell-based regenerative medicine is a promising approach for tissue reconstruction. Here, we showed that pro-inflammatory T cells in the recipients inhibited bone marrow mesenchymal stem cell (BMMSC)-mediated bone formation *via* T helper 1 (Th1) cytokine interferon (IFN)-γ induced down-regulation of runt-related transcription factor 2 (Runx-2) pathway and tumor necrosis factor (TNF)-α-regulated BMMSC apoptosis. TNF-α converted IFN-γ-activated non-apoptotic Fas to a caspase 3/8-associated apoptotic signaling in BMMSCs through inhibition of nuclear factor kappa B (NFκB), resulting in BMMSC apoptosis. Conversely, reduction of IFN-γ and TNF-α levels by systemic infusion of $Foxp3^+$ regulatory T cells (Tregs) markedly improved BMMSC-based bone regeneration and calvarial defect repair in C57BL6 mice. Furthermore, we showed that local administration of aspirin reduced levels of IFN-γ and TNF-α at the implantation site and significantly improved BMMSC-based calvarial defect repair. These data collectively uncover a previously unrecognized role of recipient T cells in BMMSC-based tissue engineering.

*Corresponding Author: Songtao Shi (songtaos@usc.edu).

AUTHOR CONTRIBUTIONS

Y.L. and L.W. performed the majority of the experiments, analyzed data and prepared the manuscript. T.K. maintained mice and helped with the *in vivo* bone formation assay. K.A. and C.C helped with cell apoptosis assay. X.X. helped with the flow cytometric analysis. R.Y. helped with *in vivo* experiments. W.J. and S.W. provided suggestions for the project. S.S. supervised the project and wrote the manuscript.

COMPETING INTERESTS STATEMENT

The authors declare that they have no competing interests.

Bone marrow mesenchymal stem cells (BMMSCs) are non-hematopoietic multipotent stem cells capable of differentiating into both mesenchymal and non-mesenchymal cell types, including osteoblasts, adipocytes, and chondrocytes[1–5]. To date, a variety of preclinical and clinical studies have shown that BMMSCs can generate bone and bone-associated tissues to replace damaged and diseased tissues, of which recipient cellular components may actively participate in the regeneration process[6–9]. However, the detailed function of recipient cells especially immune cells in BMMSC-based tissue regeneration remains unclear [9].

Previous studies demonstrated that BMMSCs reduce inflammatory cytokines *via* interplaying with several subsets of immune cells[10]. The immunoregulatory capacity of BMMSCs makes them of great interest for clinical applications in treating a variety of human diseases such as acute graft-versus-host-disease, systemic lupus erythematosus, and ameliorating hematopoietic stem cell engraftment[11–13]. Conversely, interleukin-2 (IL-2) activated NK cells and CD3/CD28-activated T cells can induce BMMSC apoptosis *via* the Fas/Fas-L pathway[14,15]. Thus, the crosstalk between implanted donor BMMSCs and recipient immune cells may play an important role in BMMSC-mediated tissue regeneration. We show in this study that recipient immune cells, specifically T cells, govern BMMSC-based tissue regeneration.

RESULTS

Recipient T cells modulated BMMSC-mediated bone regeneration

Using an established *in vivo* BMMSC implantation system, in which 4×10^6 BMMSCs with carrier hydroxyapatite tricalcium phosphate (HA/TCP) particles were subcutaneously implanted into C57BL6 or nude mice (Fig. 1a), we showed that autologous BMMSCs failed to regenerate bone in C57BL6 mice (Supplementary Fig. 1). In contrast, when BMMSCs were implanted into T cell-deficient nude mice, they formed bone and associated hematopoietic marrows (Fig. 1b). To examine whether recipient T cells affected BMMSC-mediated bone formation, we infused 1×10^6 pan-T cells into nude mice 2 days prior to subcutaneous BMMSC implantation and found that BMMSC-mediated bone formation was completely blocked (Fig. 1b). These data indicate that recipient T cells may play a crucial role in inhibiting BMMSC-mediated bone formation.

Next, we examined if specific subsets of T cells blocked BMMSC-based bone regeneration. We revealed that intravenous infusion of 1×10^6 $CD8^+$ T cells partially blocked BMMSC-mediated bone formation, and $CD4^+$ or $CD4^+CD25^-$ T cell-infusion totally blocked BMMSC-mediated bone formation in nude mice (Fig. 1b,c). However, administration of $CD4^+CD25^+Foxp3^+$ cells (Tregs) showed no inhibitive effect on BMMSC-mediated bone formation but improved bone marrow element formation (Fig. 1b,c). After systemic infusion of $CD4^+$ T cells to nude mice, we detected a transient elevation of $CD4^+$ T cell level in bone marrow, peripheral blood, and spleen within 7 days post infusion (Supplementary Fig. 2a–c) and infused $CD4^+$ T cells at areas around BMMSC implants (Supplementary Fig. 2d). Furthermore, we revealed that BMMSC-mediated bone formation started at 14 days post implantation and substantial amount of bones were formed at 21 days post implantation (Supplementary Fig. 3).

To explore mechanisms of T cell-regulated BMMSC-based bone formation, we assessed the levels of a variety of cytokines, including IFN-γ, TNF-α, IL-4, IL-6, and IL-17A in the BMMSC implants (Fig. 1d). Interestingly, the levels of IFN-γ and TNF-α in BMMSC implants were significantly elevated at 7–14 days after BMMSC implantation in C57BL6 mice and nude mice receiving pan-T cell or $CD4^+CD25^-$ T cells (Fig. 1d). The high levels of IFN-γ and TNF-α were correlated with lack of new bone formation (Fig. 1b,c). Conversely, the levels of above mentioned cytokines were not altered in the BMMSC implants derived from nude and Treg-infused nude mice (Fig. 1d); these implants showed substantial amount of new bone formation (Fig. 1b,c). Thus, the increase in IFN-γ and TNF-α is negatively correlated with BMMSC-mediated bone formation.

To further assess the role of cytokines in BMMSC-mediated bone formation, 200 ng of IFN-γ, TNF-α, IL-4, IL-6, or IL-17A was co-implanted with BMMSCs into nude mice subcutaneously (Fig. 1e,f). Treatment with IFN-γ or TNF-α significantly reduced BMMSC-mediated bone in nude mice (Fig. 1e,f). Meanwhile, IL-4 or IL-6 treatment slightly inhibited BMMSC-mediated bone formation (Fig. 1e,f), and IL-17A treatment had no inhibitory effect on BMMSC-mediated bone formation when compared to the untreated group (Fig. 1e,f). Neutrophils presented at BMMSC implants at 2 to 7 days post implantation and became almost undetectable after 14 days implantation in C56BL6 mice (Supplementary Fig. 4a). At areas around BMMSC implant, $CD4^+$ T cells produced IFN-γ and TNF-α, $CD11b^+$ macrophages only produced TNF-α (Supplementary Fig. 4b). In contrast, injection of IFN-γ neutralizing antibody at 150 and 300 ng and TNF-α neutralizing antibody at 300 ng partially rescued BMMSC-mediated bone formation in C57BL6 mice (Fig. 1g,h). Injection of combination of IFN-γ and TNF-α neutralizing antibodies at 300 ng could significantly improve BMMSC-mediated bone formation (Fig. 1g,h). These data confirm that both IFN-γ and TNF-α played critical roles in governing BMMSC-based bone formation.

$CD4^+CD25^+Foxp3^+$ Tregs have been reported to inhibit T cell activation and reduce IFN-γ and TNF-α production[16–19]. Thus, we infused 1×10^6 Tregs into C57BL6 mice either 2 or 7 days prior to the BMMSC implantation and found substantial amount of bone formation in group of Treg-infused at 2 days prior BMMSC implantation as compared to untreated BMMSC implants (Fig. 2a,b). Treg infusion at 7 days prior BMMSC implantation failed to improve bone formation in BMMSC implants (Fig. 2a,b). To examine the protective role of Tregs in BMMSC-based bone formation, we measured the cytokine levels in the Treg-treated C57BL6 mice. We observed that Tregs infusion reduced the levels of IFN-γ and TNF-α, but not the levels of IL-4 and IL-10 (Fig. 2c) in BMMSC implants. Subcutaneous implantation of BMMSCs failed to affect the level of Tregs in spleen (Fig. 2d). Systemic infusion of Tregs and BMMSCs elevated levels of Tregs in spleen, which reduced to control level at 14 days post infusion (Fig. 2e,f). Infusion of 1×10^6 and 2×10^6 Tregs showed more significant elevation of Tregs in spleen than 0.1×10^6 and 0.5×10^6 Treg groups (Fig. 2g). Accordingly, infusion of 1×10^6 and 2×10^6 Tregs, but not 0.1×10^6 and 0.5×10^6 groups, were able to improve BMMSC-mediated bone formation in C57BL6 mice (Fig. 2h,i). These data collectively suggest that inhibition of IFN-γ and TNF-α improves BMMSC-based bone regeneration.

IFN-γ inhibited osteogenesis of BMMSCs

When *Ifn-γ*$^{-/-}$ T cells were infused into nude mice, they failed to block BMMSC-mediated bone formation (Supplementary Fig. 5a–c). Further analysis showed that *in vitro* IFN-γ (200 ng ml^{-1}), but not IL-6 or IL-17A, treatment inhibited osteogenic differentiation of BMMSCs compared to untreated groups (Fig. 3a). IL-4 treatment (200 ng ml^{-1}) served as a control showing the inhibition of BMMSC osteogenic differentiation *in vitro*[20] (Fig. 3a). Interestingly, 50 ng ml^{-1} IFN-γ treatment had no inhibitory effect on osteogenic differentiation of BMMSCs (Fig. 3b). The dose-dependent osteogenic inhibition by IFN-γ was associated with up-regulated expression of Smad 6, a negative regulator of osteogenic differentiation, and down-regulated expression of the osteogenic genes runt-related transcription factor 2 (Runx2), osteocalcin (OCN), and alkaline phosphatase (ALP) in 200 ng ml^{-1} IFN-γ group, which were not observed in 50 ng ml^{-1} IFN-γ group (Fig. 3c). Furthermore, we revealed that IFN-γ treatment failed to suppress osteogenic differentiation and alter expression levels of Smad 6 and Runx2 in *Fas*$^{-/-}$ BMMSCs (Fig. 3d) and *Fas* knockdown BMMSCs by siRNA (Fig. 3e).

IFN-γ synergistically enhanced TNF-α-induced BMMSC apoptosis

When BMMSCs were cultured with IFN-γ, TNF-α, IL-4, IL-6, IL-17A, and TGF-β, only TNF-α induced a significant cell death in a dose-dependent manner (Fig. 4a). To determine the effect of IFN-γ on TNF-α-treated BMMSCs, we added 50 ng ml^{-1} IFN-γ to BMMSCs that were treated with different doses of TNF-α (1–200 ng ml^{-1}; Fig. 4b). IFN-γ treatment significantly enhanced BMMSC apoptosis when the TNF-α concentration reached 50–200 ng ml^{-1} (Fig. 4b; Supplementary Fig. 5d,e). To further confirm the synergistic effects of TNF-α and IFN-γ on the induction of BMMSC apoptosis, we added 50 ng ml^{-1} TNF-α to BMMSCs that were treated with 1–200 ng ml^{-1} IFN-γ (Fig. 4c). The amount of BMMSC apoptosis was correlated with IFN-γ concentration from 1–50 ng ml^{-1}. When IFN-γ concentration reached 100–200 ng ml^{-1}, a complete BMMSC apoptosis was observed (Fig. 4c). In addition, we used immunocytostaining with annexin V to confirm that 50 ng ml^{-1} IFN-γ enhanced 20 ng ml^{-1} TNF-α-mediated BMMSC apoptosis (Fig. 4d). Next, we verified the IFN-γ synergic effect on TNF-α-induced BMMSC apoptosis using an *in vivo* subcutaneous GFP^{+} BMMSC implantation model[21,22]. Thirty days after implantation, GFP^{+} BMMSCs that were pre-treated with 50 ng ml^{-1} TNF-α showed a significant reduction in the numbers of surviving cells than those from untreated group (Fig. 4e). Combination treatment with 200 ng ml^{-1} IFN-γ and 50 ng ml^{-1} TNF-α led to no survival of GFP^{+} BMMSCs in the implants (Fig. 4e). These data indicate that IFN-γ is capable of synergistically enhancing TNF-α-induced BMMSC apoptosis.

We next found that IFN-γ treatment up-regulated Fas expression in BMMSCs without activating caspase 3 and caspase 8 (Fig. 4f, Supplementary Fig. 5f). With the addition of 20 ng ml^{-1} TNF-α, a concentration unable to induce marked BMMSC apoptosis, to 50 ng ml^{-1} IFN-γ-treated BMMSCs, caspase 3 and caspase 8 were activated (Fig. 4f, Supplementary Fig. 6a) along with significant BMMSC apoptosis (Fig. 4h). However, combination of 20 ng ml^{-1} TNF-α and 50 ng ml^{-1} IFN-γ treatment failed to activate caspase 3 and caspase 8 in *Fas*$^{-/-}$ BMMSCs (Fig. 4f). Furthermore, we used siRNA to knockdown Fas expression in BMMSCs and showed that activated caspase 8 and caspase 3 were partially blocked in IFN-

γ/TNF-α treated BMMSCs (Fig. 4g) with a significant reduction in the number of apoptotic BMMSCs (Fig. 4h). These data suggest that Fas signaling is required for the IFN-γ synergistic effect on TNF-α-induced BMMSC apoptosis.

Next question we asked is how Fas apoptotic signaling was activated in IFN-γ/TNF-α-treated BMMSCs. We revealed that knockdown Fas-L level using siRNA in IFN-γ/TNF-α-treated BMMSCs was not able to reduced number of apoptotic cells (Supplementary Fig. 6b), excluding Fas-L as a potential factor contributing to BMMSC apoptosis. We showed that combined treatment of IFN-γ and TNF-α induced Fas internalization and clustering. In untreated control group, Fas was evenly distributed on BMMSC surface (Fig. 5a). BMMSCs were treated with IFN-γ for 12 hours and then TNF-α was added, Fas showed marked clustering and internalization in cytoplasm at 0.5–1 hour (Fig. 5a). Significant Fas clustering in combination with cell shrinkage and cell membrane disruption was observed at 2–4 hours following TNF-α treatment (Fig. 5a). Blockage of Fas internalization by endocytosis inhibitor Latrunadin A (LntA) partially rescued IFN-γ/TNF-α-induced BMMSC apoptosis with inhibition of cleaved caspase 3 and 8 (Fig. 5b). Interestingly, with blocking caspase 8 or caspase 3 activities using their specific inhibitors, IFN-γ/TNF-α-treated BMMSCs exhibited significant reduction in the number of apoptotic cells (Fig. 5c). Moreover, inhibition of pan caspase, caspase 3, and caspase 8 was able to partially block Fas internalization (Fig. 5d). These data suggest that Fas internalization and clustering contribute to synergistic BMMSC apoptosis *via* activation of caspase 8/3 in the presence of IFN-γ and TNF-α.

We next investigated how combination of IFN-γ and TNF-α resulted in Fas internalization and clustering in BMMSCs. First, we showed that IFN-γ/TNF-α treatment could not induce up-regulation of TNFR1, TRAIL, and Fas L proteins (Supplementary Fig. 6c). Then we found that IFN-γ/TNF-α treatment reduced levels of TNFR2 and its downstream signaling phosphorylated NF-κB, XIAP, and FLIP (Fig. 5e), suggesting that combination of IFN-γ and TNF-α treatment selectively inhibited TNFR2-mediated anti-apoptotic effect. To confirm this hypothesis, we showed that reduction of TNFR2, IKK, XIAP, and FLIP by siRNA further activated caspase 8 and 3 (Fig. 5f). The efficiency of TNFR2, IKK, XIAP, and FLIP knockdown by their specific siRNAs was confirmed by Western blot analysis (Supplementary Fig. 6d).

These findings collectively revealed that IFN-γ treatment activated Fas expression levels in BMMSCs and initiated a non-apoptotic pathway, in which osteogenesis was inhibited by activation of Smad 6 (Supplementary Fig. 7a). Treatment of BMMSCs with IFN-γ and TNF-α together, however, was able to convert the non-apoptotic Fas signaling to a death pathway (Supplementary Fig. 7b).

Treg treatment improved BMMSC-based repair of calvarial defects

Since infusion of Tregs inhibited levels of TNF-α and IFN-γ (Fig. 2c), we hypothesized that Treg treatment improves cell-based tissue engineering. To test this hypothesis, we generated critical-sized calvarial bone defects (7 × 8 mm; Fig. 6a,b). Very small amounts of bone formation were observed in the untreated group at 12 weeks after surgery (Fig. 6b). Implantation of BMMSC/gelfoam at calvarial defect site showed moderate bone

regeneration, but failed to completely repair the defects (Fig. 6c). However, infusion of Tregs into the recipients 2 days prior to BMMSC/gelfoam implantation resulted in complete repair of the defects (Fig. 6d). Semi-quantitative analysis showed the amount of calvarial bone regeneration in each group (Fig. 6e). The regenerated bone structure in BMMSC+Treg group was identical to the control with a completely suture regeneration (Fig. 6a,d). These data imply that Treg treatment improves BMMSC-mediated calvarial defect repair.

Site-specific aspirin treatment improved BMMSC-based repair of calvarial defects

Next, we investigated whether site-specific pharmacological treatments would improve BMMSC-based calvarial defect repair. Since aspirin has been reported to inhibit the function of TNF-α and IFN-γ[23], we examined the effect of aspirin treatment on IFN-γ and TNF-α levels in BMMSC implants at 2–14 days after implantation. We showed that aspirin treatment reduced the levels of IFN-γ and TNF-α without affecting IL-10 level (Supplementary Fig. 8). When added to BMMSC/activated T cell co-culture system, aspirin at 25, 50, and 100 μg ml^{-1} was able to significantly reduce levels of IFN-γ and TNF-α (Supplementary Fig. 9). Immunohistochemical analysis confirmed the inhibitory effect of aspirin evidenced by the reduction in the number of IFN-γ and TNF-α positive cells in BMMSC implants (Fig. 6f). To determine if aspirin-mediated reduction of IFN-γ or TNF-α in BMMSC implants influenced the apoptosis of BMMSCs, we utilized a GFP^+ BMMSC implantation model which revealed a significant increase in survival of BMMSCs in aspirin-treated group during 4–30 days post implantation (Supplementary Fig. 10a).

Next, we studied the effect of aspirin on inhibition of exogenous IFN-γ and TNF-α on BMMSC-mediated bone formation. We treated BMMSCs with 50 μg ml^{-1} aspirin for 2 days followed by subcutaneous implantation into nude mice using HA/TCP as a carrier. The aspirin pre-treatment increased BMMSC-mediated bone formation compared to the untreated group (Supplementary Fig. 10b,c). We then implanted BMMSC with IFN-γ or TNF-α (200 ng) and observed a significantly reduced bone formation (Fig. 1e,f; Supplementary Fig. 10d,e). However, addition of aspirin (100 μg) to BMMSC implants restored bone formation that was suppressed by IFN-γ or TNF-α (Supplementary Fig. 10f–h). Moreover, we showed that implantation of BMMSC/hydrogel/aspirin (25–200 μg), along with BMMSC/gelfoam/aspirin (100 μg), (Supplementary Fig. 11) resulted in a dose dependent improvement of bone regeneration in calvarial defect area compared to the control BMMSC group (Fig. 6g,h). The structures of regenerated tissues were analogous to normal calvarial tissues with a completely suture regeneration at 100 and 200 μg groups (Fig. 6g,h).

DISCUSSION

The clinical use of culture-expanded osteoprogenitor cells in conjunction with scaffolds has been reported for tissue engineering[24–26]. However, the main challenge of cell-based tissue regeneration is to form large quantities and high-quality tissue structures that match the body's functional needs[27,28]. In this study, we developed a practical approach to improve BMMSC-based tissue engineering through suppression of IFN-γ and TNF-α by a site-specific aspirin treatment.

In addition to IFN-γ and TNF-α induced BMMSC apoptosis, other immune cell-based regulatory mechanisms may also contribute to the cell apoptosis in BMMSC implants. CD3-activated T lymphocytes are capable of inducing BMMSC apoptosis in a direct cell co-culture system through Fas/Fas ligand pathway[15,29]. Also, T cells can induce BMMSC/osteoblast apoptosis *via* CD40/CD40L pathway as observed in some bone-related disease models[30–33]. Further studies are required to elucidate whether donor BMMSC apoptosis attributes to Fas/Fas ligand and CD40/CD40L pathways.

It is unknown how IFN-γ elevates Fas expression level in BMMSCs, and other cells such as osteosarcoma cell lines[34]. Interestingly, IFN-γ-induced Fas expression associated with IFN-γ-mediated blockage of osteogenic differentiation of BMMSCs by activating Smad-6 pathway. It was known that Smad-6 inhibits osteogenic differentiation *via* BMP and runx2 signaling[35,36]. However, a relatively high concentration of IFN-γ was required to inhibit the osteogenesis of BMMSCs. Therefore, the inhibitory function of IFN-γ in BMMSC-mediated bone formation was likely due to the synergistic effect with TNF-α, which resulted in enhanced BMMSC apoptosis by activation of Fas signaling-mediated death pathway. In this regard, IFN-γ treatment alone can up-regulate Fas expression, but fails to induce BMMSC apoptosis, which might be attributed to the anti-apoptotic function of TNFR2-associated NFκB, XIAP, and FLIP in this cascade[37,38]. With the addition of TNF-α treatment, however, IFN-γ-induced non-apoptotic Fas signaling was converted to an apoptotic cascade due to the reduction of anti-apoptotic factors NFκB, XIAP, and FLIP as evidenced by Fas internalization and activation of death mediators caspase 3 and 8.

Aspirin is a widely used nonsteroidal anti-inflammatory agent (NSAID). It inhibits osteoclastogenesis, and improves osteogenesis by affecting multiple biological pathways, such as inhibition of COX2, COX1, and PGE2 activity[15,23,39]. Epidemiological study suggests that aspirin may have a moderate beneficial effect on bone mineral density in postmenopausal woman[15]. In animal model study, aspirin treatment improves bone formation and inhibits bone resorption in OVX-induced osteoporotic mice, which may associate with aspirin-induced up-regulation of telomerase in BMMSCs[15,40]. In this study, we showed that aspirin suppressed the levels of TNF-α and IFN-γ and reversed the proinflammatory cytokine-induced osteogenic deficiency of BMMSCs. We further used subcutaneous implantation and a calvarial bone defect repair model to show that aspirin treatment is an appropriate approach for improving BMMSC-based tissue regeneration by suppression of IFN-γ and TNF-α. Although aspirin reduces TNF-α and IFN-γ production with improving BMMSC-based tissue regeneration, the therapeutic effect of aspirin in pre-clinical test and clinical trial such as improving fracture healing may be the focus of future studies.

METHODS

Animals

Female C3H/HeJ, C57BL6J, B6.129S7-*Ifng*^{tm1Ts}/J, C57BL/6-Tg(CAG-EGFP)1Osb/J, B6.MRL-*Fas*^{lpr}/J mice were purchased from Jackson Lab. Female immunocompromised nude mice (Beige *nude*/*nude* XIDIII) were purchased from Harlan. All animal experiments

were performed under the institutionally approved protocols for the use of animal research (University of Southern California protocols #10874 and 10941).

BMMSC-mediated bone formation

Approximately 4.0×10^6 BMMSCs were mixed with hydroxyapatite/tricalcium phosphate (HA/TCP) ceramic particles (40 mg, Zimmer Inc.) as a carrier and subcutaneously implanted into the dorsal surface of 8–10 weeks old nude mice or C57BL6J mice. At eight weeks post-implantation, the implants were harvested. Hematoxylin and eosin staining of histological section was analyzed by NIH Image J.

Cytokines in BMMSC-mediated bone formation

BMMSCs were mixed with HA/TCP ceramic powders, and Extracel-HP™ hydrogel (Glycosan Biosysterms) containing 200 ng IFN-γ, TNF-α, IL-4, IL-6 or IL-17A were covered on the surface of the implants for slow release of the cytokines. At eight weeks post–implantation, the implants were harvested and newly formed mineralized tissue areas were analyzed. The cytokine levels in the implants were measured by ELISA kit.

Cell apoptosis and cell survival assay

0.5×10^6 BMMSCs were seeded to 6-well culture plates and co-cultured with different doses of recombined IL-4, IL-6, IL-17A, TGF-β1, TNF-α and IFN-γ (0, 10, 20, 50, 100, 200 ng ml^{-1}) for 3 days. To measure cell viability, total cells were analyzed by using a cell counting kit-8 (Dojindo Molecular Technoloies). The culture plates were stained with 2% toluidine blue O and 2% paraformaldehyde. For cell apoptosis analysis, BMMSCs were stained by Annexin V-PE apoptosis detection kit I (BD Bioscience), and analyzed by FACS^{Calibur} (BD Bioscience).

IFN-γ and TNF-α synergism for apoptosis

1×10^4 BMMSCs were seeded to 2-chamber slides, IFN-γ (50 ng ml^{-1}) and TNF-α (20 ng ml^{-1}) were used to treat the BMMSCs for 24 hours either separately or combined. Annexin V-PE apoptosis detection kit I and cell counting kit were used for analysis.

Cell survival assay *in vivo*

4×10^6 BMMSCs isolated from C57BL/6-Tg (CAG-EGFP)1Osb/J mice were combined with different concentrations of IFN-γ and TNF-α (0, 20, 50, 100, 200 ng ml^{-1}) and subcutaneously transplanted into nude mice, hydrogel was used as a slowly released carrier. Thirty days after translation, the implants were harvested. The cells in implants were cultured for 10 days, and GFP positive cell numbers were counted under fluorescent microscopy.

$CD4^+CD25^+Foxp3^+$ Tregs induction

To induce $CD4^+CD25^+Foxp3^+$ Tregs *in vitro*, $CD4^+CD25^-$ T lymphocytes were collected by $CD4^+CD25^+$ regulatory T Cell Isolation Kit (Miltenyi Biotec), and 1×10^6 $CD4^+CD25^-$ T lymphocytes in each well were cultured with 1 μg ml^{-1} plate-bounded antibody to CD3ε, 2 μg ml^{-1} soluble antibody to CD28, recombinant mouse TGF-β1 (2 μg ml^{-1}) (R&D

Systems) and recombinant mouse IL2 (2 μg ml^{-1}) (R&D Systems) for 3 days. Then, $CD4^+CD25^+$ T lymphocytes were isolated using $CD4^+CD25^+$ regulatory T Cell Isolation Kit.

Fas internalization

BMMSCs were seeded to 2-well chamber slides. IFN-γ (50 ng ml^{-1}) was added to pre-treat BMMSCs for 24 hours, and then TNF-α (20 ng ml^{-1}) was added. At 0.5, 1, 2, 4 hours after TNF-α was added, the cells fixed with 4% PFA for 15 min. After treated by Triton-X for 15 min, the cells were incubated with 1 μg ml^{-1} Fas specific antibody (Santa Cruz) at room temperature for 2 hours, treated with Rhodamin–conjugated secondary antibodies (1:200, Jackson ImmunoResearch). Then the cells were incubated with α-actin (1:40, Invitrogen) at room temperature for 20 min and mounted.

Implantation of BMMSCs to calvarial bone defects in C57BL6J mice

7 × 8 mm oversize bone defects were established on calvarial bones of C57BL6J mice. 4×10^6 BMMSCs were treated with different dose of aspirin (25, 50, 100, 200 μg ml^{-1}) for 3 days and mixed with 200 μl hydrogel. The hydrogel/BMMSCs with aspirin (25, 50, 100, 200 μg in each implant) were transplanted to newly generated calvarial bone defects (Supplementary Fig. 11). 2×10^6 BMMSCs were seeded to gelfoam (7 × 8 mm, Pharmaca) and cultured for 3 days *in vitro* with different dose of aspirin (25, 50, 100, 200 μg ml^{-1}). The gelfoam/BMMSCs containing aspirin (25, 50, 100, 200 μg in each implant) were used to cover previous implanted BMMSC/hydrogel complex in the calvarial bone defect area (Supplementary Fig. 11). No aspirin was added in control group. The calvarial bone defects were completely covered with skin and sutured.

Statistics

SPSS 13.0 was used to do statistical analysis. Significance was assessed by independent two-tailed Student's *t*-test or analysis of variance (ANOVA). The *P* values less than 0.05 were considered significant.

Additional methods

Detailed methodology is described in the Supplementary Methods online.

Supplementary Material

Refer to Web version on PubMed Central for supplementary material.

Acknowledgments

We thank Dr. Xiaohong Duan and Mr. Tao Zhou of Fourth Military Medical University to generate microCT images. This work was supported by grants from National Institute of Dental and Craniofacial Research, National Institutes of Health, Department of Health and Human Services (R01DE017449, R01DE019932, and R01DE019413 to S.S.), grant from California Institute for Regenerative Medicine (RN1-00572 for S.S.), and Intramural program of National Institute of Dental and Craniofacial Research, National Institutes of Health, Department of Health and Human Services.

References

1. Bianco P, Riminucci M, Gronthos S, Robey PG. Bone marrow stromal stem cells: nature, biology, and potential applications. Stem Cells. 2001; 19:180–192. [PubMed: 11359943]
2. Friedenstein AJ, Chailakhyan RK, Latsinik NV, Panasyuk AF, Keiliss-Borok IV. Stromal cells responsible for transferring the microenvironment of the hemopoietic tissues. Cloning *in vitro* and retransplantation *in vivo*. Transplantation. 1974; 17:331–340. [PubMed: 4150881]
3. Owen M, Friedenstein AJ. Stromal stem cells: marrow-derived osteogenic precursors. Ciba Found Symp. 1988; 136:42–60. [PubMed: 3068016]
4. Pittenger MF, et al. Multilineage potential of adult human mesenchymal stem cells. Science. 1999; 284:143–147. [PubMed: 10102814]
5. Prockop DJ. Marrow stromal cells as stem cells for nonhematopoietic tissues. Science. 1997; 276:71–74. [PubMed: 9082988]
6. Caplan AI. Adult mesenchymal stem cells for tissue engineering versus regenerative medicine. J Cell Physiol. 2007; 213:341–347. [PubMed: 17620285]
7. Garcia-Gomez I, et al. Mesenchymal stem cells: biological properties and clinical applications. Expert Opin Biol Ther. 2010; 10:1453–1468. [PubMed: 20831449]
8. Tasso R, Fais F, Reverberi D, Tortelli F, Cancedda R. The recruitment of two consecutive and different waves of host stem/progenitor cells during the development of tissue-engineered bone in a murine model. Biomaterials. 2010; 31:2121–2129. [PubMed: 20004968]
9. Bueno EM, Glowacki J. Cell-free and cell-based approaches for bone regeneration. Nat Rev Rheumatol. 2009; 5:685–697. [PubMed: 19901916]
10. Zhao S, et al. Immunomodulatory properties of mesenchymal stromal cells and their therapeutic consequences for immune-mediated disorders. Stem Cells Dev. 2010; 19:607–614. [PubMed: 19824807]
11. Tolar J, Le Blanc K, Keating A, Blazar BR. Concise review: hitting the right spot with mesenchymal stromal cells. Stem Cells. 2010; 28:1446–1455. [PubMed: 20597105]
12. English K, French A, Wood KJ. Mesenchymal stromal cells: facilitators of successful transplantation? Cell Stem Cell. 2010; 7:431–442. [PubMed: 20887949]
13. Sun L, et al. Mesenchymal stem cell transplantation reverses multi-organ dysfunction in systemic lupus erythematosus mice and humans. Stem Cells. 2009; 27:1421–1432. [PubMed: 19489103]
14. Spaggiari GM, Capobianco A, Becchetti S, Mingari MC, Moretta L. Mesenchymal stem cell-natural killer cell interactions: evidence that activated NK cells are capable of killing MSCs. whereas MSCs can inhibit IL-2-induced NK-cell proliferation. Blood. 2006; 107:1484–1490. [PubMed: 16239427]
15. Yamaza T, et al. Pharmacologic stem cell based intervention as a new approach to osteoporosis treatment in rodents. PLoS ONE. 2008; 3:e2615. [PubMed: 18612428]
16. Lourenco EV, La Cava A. Natural regulatory T cells in autoimmunity. Autoimmunity. 2011; 44:33–42. [PubMed: 21091291]
17. Zhou X, et al. Therapeutic potential of TGF-beta-induced CD4(+) Foxp3(+) regulatory T cells in autoimmune diseases. Autoimmunity. 2011; 44:43–50. [PubMed: 20670119]
18. Shevach EM. $CD4^+CD25^+$ suppressor T cells: more question than answers. Nat Rev Immunol. 2002; 2:389–400. [PubMed: 12093005]
19. van Mierlo GJ, et al. Cutting edge: TNFR-shedding by $CD4^+CD25^+$ regulatory T cells inhibits the induction of inflammatory mediators. J Immunol. 2008; 180:2747–2751. [PubMed: 18292492]
20. Ura K, et al. Interleukin (IL)-4 and IL-13 inhibit the differentiation of murine osteoblastic MC3T3-E1 cells. Endocr J. 2000; 47:293–302. [PubMed: 11036873]
21. Krebsbach PH, et al. Bone formation in vivo: comparison of osteogenesis by transplanted mouse and human marrow stromal fibroblasts. Transplantation. 1997; 63:1059–1069. [PubMed: 9133465]
22. Batouli S, et al. Comparison of stem cell-mediated osteogenesis and dentinogenesis. J Den Res. 2003; 82:975–980.
23. Kwon MS, et al. Effect of aspirin and acetaminophen on proinflammatory cytokine-induced pain behavior in mice. Pharmacology. 2005; 74:152–156. [PubMed: 15775706]

24. Kwan MD, Slater BJ, Wan DC, Longaker MT. Cell-based therapies for skeletal regenerative medicine. Hum Mol Genet. 2008; 17:R93–98. [PubMed: 18632703]
25. Panetta NJ, Gupta DM, Quarto N, Longaker MT. Mesenchymal cells for skeletal tissue engineering. Panminerva Med. 2009; 51:25–41. [PubMed: 19352307]
26. Fredericks DC, et al. Cellular interactions and bone healing responses to a novel porous tricalcium phosphate bone graft material. Orthopedics. 2004; 27:s167–173. [PubMed: 14763552]
27. Seong JM, et al. Stem cells in bone tissue engineering. Biomed Mater. 2010; 5:062001. [PubMed: 20924139]
28. Undale AH, Westendorf JJ, Yaszemski MJ, Khosla S. Mesenchymal stem cells for bone repair and metabolic bone diseases. Mayo Clin Proc. 2009; 84:893–902. [PubMed: 19797778]
29. Kogianni G, Mann V, Ebetino F, et al. Fas/CD95 is associated with glucocorticoid-induced osteocyte apoptosis. Life Sci. 2004; 75:2879–2895. [PubMed: 15454340]
30. Hess S, Engelmann H. A novel function of CD40: induction of cell death in transformed cells. J Exp Med. 1996; 183:159–167. [PubMed: 8551219]
31. Li JY, et al. Ovariectomy disregulates osteoblast and osteoclast formation through the T-cell receptor CD40 ligand. Proc Natl Acad Sci U S A. 2011; 108:768–773. [PubMed: 21187391]
32. Ahuja SS, Zhao S, Bellido T, Plotkin LI, Jimenez F, Bonewald LF. CD40 ligand blocks apoptosis induced by tumor necrosis factor alpha, glucocorticoids, and etoposide in osteoblasts and the osteocyte-like cell line murine long bone osteocyte-Y4. Endocrinology. 2003; 144:1761–1769. [PubMed: 12697681]
33. Schrum LW, Marriott I, Butler BR, Thomas EK, Hudson MC, Bost KL. Functional CD40 expression induced following bacterial infection of mouse and human osteoblasts. Infect Immun. 2003; 71:1209–1216. [PubMed: 12595434]
34. Li Z, et al. IFN-γ enhances HOS and U2OS cell lines susceptibility to γδ T cell-mediated killing through the Fas/Fas ligand pathway. Int Immunopharmacol. 2011; 11:496–503. [PubMed: 21238618]
35. Shen R, et al. Smad6 intereacts with Runx2 and mediates Smad ubiquitin regulatory factor 1-induced Runx2 degradation. J Biol Chem. 2006; 281:3569–3576. [PubMed: 16299379]
36. Itoh F, et al. Promoting bone morphogenetic protein signaling through negative regulation of inhibitory Smads. EMBO J. 2001; 20:4132–4142. [PubMed: 11483516]
37. Qin JZ, et al. Role of NF-κB in the apoptotic-resistant phenotype of keratinocytes. J Biol Chem. 1999; 274:37957–37964. [PubMed: 10608863]
38. Moon DO, Kim MO, Kang SH, Choi YH, Kim GY. Sulforaphane suppresses TNF-alpha-mediated activation of NF-kappaB and induces apoptosis through activation of reactive oxygen species-dependent caspase-3. Cancer Lett. 2009; 274:132–142. [PubMed: 18952368]
39. Buckland M, et al. Aspirin-treated human DCs up-regulate ILT-3 and induce hyporesponsiveness and regulatory activity in responder T cells. Am J Transplant. 2006; 6:2046–2059. [PubMed: 16869801]
40. Shi S, et al. Bone formation by human postnatal bone marrow stromal stem cells is enhanced by telomerase expression. Nat Biotechnol. 2002; 20:587–591. [PubMed: 12042862]

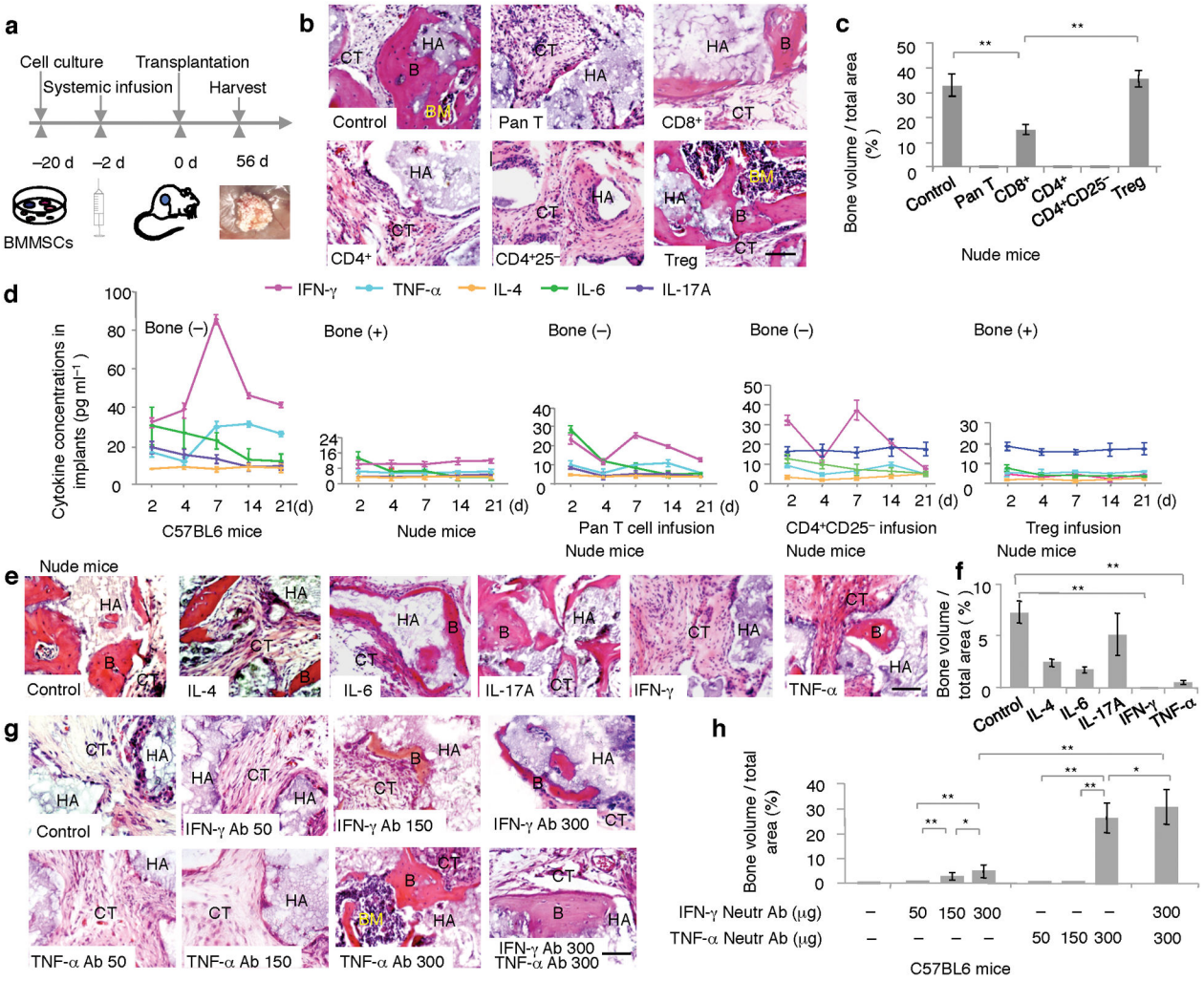

Figure 1. T cells regulated BMMSC-mediated bone formation

(**a**) Scheme of assessing BMMSC-based tissue regeneration. **(b)** Subcutaneous implantation of mouse BMMSCs in nude mice formed substantial amount of bone (B), bone marrow (BM), and connective tissue (CT) around hydroxyapaptite/tricalcium phosphate (HA/TCP, HA) at 8 weeks post implantation (Control). Infusion of Pan T cells (Pan T), $CD4^+$ T cells ($CD4^+$), and $CD4^+CD25^-$ T cells ($CD4^+CD25^-$) blocked BMMSC-mediated bone formation in nude mice. H&E staining showed connective tissue (CT) surround HA/TCP (HA) in the BMMSC implants. Infusion of $CD8^+$ T cells partially blocked BMMSC-mediated bone formation ($CD8^+$). Infusion of $CD4^+CD25^+Foxp3^+$ regulatory T cells (Tregs) showed no inhibitive effect on bone (B) and improvement of bone marrow (BM) formation. (**c**) Image J semi-quantitative analysis indicated amount of bone formation in BMMSC implants in nude mice. (**d**) Subcutaneous implantation of BMMSCs in C57BL6 mice elevated expression of IFN-γ and TNF-α in the BMMSC implants from 4 to 14 days post implantation as evidenced by ELISA analysis (far left panel). However, there were no significant changes in the levels of IL-4, IL-6, and IL-17A in the BMMSC implants (far left panel). Subcutaneous implantation of BMMSCs in nude mice showed no significant change in levels of IFN-γ,

TNF-α, IL-4, IL-6, and IL-17A (left panel). With infusion of Pan T cells or $CD4^+CD25^-$ cells into nude mice, the levels of IFN-γ and TNF-α were increased in BMMSC implants, along with no significant change for the levels of IL-4, IL-6, and IL-17A (middle and right panels). Infusion of Tregs appeared no effect on the levels of IFN-γ, TNF-α, IL-4, IL-6, and IL-17A in the BMMSC implants in nude mice (far right panel). (**e**) Subcutaneous implantation of IFN-γ, TNF-α, IL-4, IL-6, and IL-17A (200 ng) with hydrogel and BMMSCs in nude mice showed that BMMSC/HA/TCP positive control group had marked bone formation (B) around HA/TCP (HA) at 8 weeks post implantation (Control). IL-4 and IL-6 treated BMMSCs showed a reduction in new bone formation (IL-4, IL-6) and IL-17A treatment appeared no inhibitive effect on BMMSC-mediated bone formation (IL-17A). Moreover, IFN-γ treatment resulted in a completely blockage of new bone formation (IFN-γ) and TNF-α treatment led to a very limited bone formation in BMMSC implants (TNF-α). (**f**) Image J semi-quantitative analysis showed the amount of new bone formation in each group. (**g**) When IFN-γ and TNF-α neutralizing antibodies (50, 150, 300 μg/mouse) were injected into C57BL6 mice at 2 days prior to BMMSC implantation, there is no bone formation in groups treated with 50 μg IFN-γ antibody (IFN-γ Ab 50), 50 and 150 μg TNF-α antibody (TNF-α Ab 50, TNF-α Ab 150). New bone formation was observed in 150 μg and 300 μg IFN-γ neutralizing antibody treatment groups (IFN-γ Ab 150, IFN-γ Ab 300), and 300 μg TNF-α antibody treatment groups (TNF-α Ab 300). Combination treatment of 300 μg IFN-γ and 300 μg TNF-α resulted in a marked bone formation (IFN-γ Ab 300, TNF-α Ab 300). (**h**) The amount of new bone formation was shown by semi-quantitative analysis of image J analysis. (**P* < 0.05, ***P* < 0.01, *n* = 5). Scale bar, 100μm.

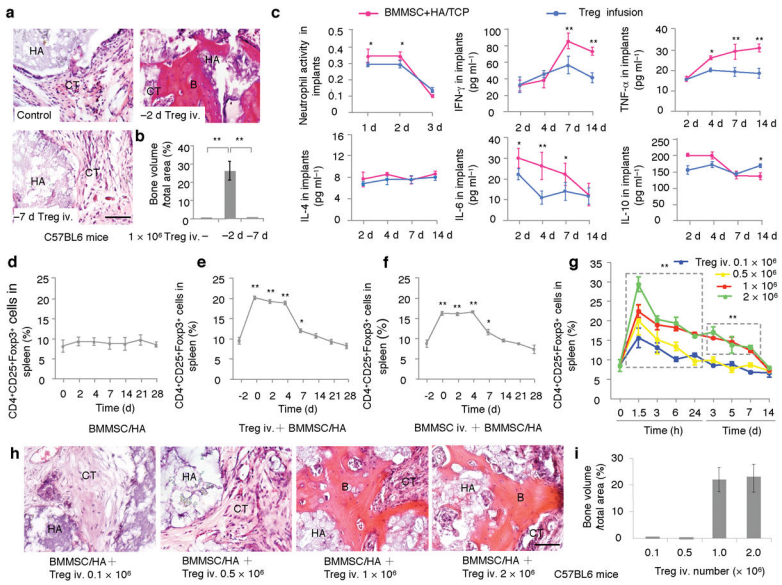

Figure 2. Regulatory T cell (Treg) improved BMMSC-mediated bone formation in C57BL6 mice

(**a)** Subcutaneous implantation of littermate BMMSCs in C57BL6 mice failed to regenerate bone at 8 weeks post implantation. H&E staining showed connective tissue (CT) surround HA/TCP (HA) in the BMMSC implants (Control). However, Infusion of $CD4^+CD25^+Foxp3^+$ regulatory T cells at 2 days prior to the BMMSC/HA/TCP implantation resulted in a marked new bone formation (B) around HA/TCP (HA) and connective tissue (CT) in BMMSC implants at 8 weeks post implantation (−2d Tregs *iv*.). Infusion of $CD4^+CD25^+Foxp3^+$ regulatory T cells at 7 days prior to the BMMSC/HA/TCP implantation failed to show bone formation (−7 d Tregs *iv*.). (**b**) Image J semi-quantitative analysis indicated relative amount of bone volume in BMMSC implants. (**c**) ELISA analysis showed that Treg infusion reduced levels of IFN-γ and TNF-α in the BMMSC implants at 7–14 days post implantation when compared to untreated control group. The levels of IL-4 and IL-10 had no significant changes among these groups. In addition, Treg infusion reduced the number of neutrophil cells and levels of IL-6 in the BMMSC implants at 1–2 and 4–7 days post implantation, respectively. **(d)** Subcutaneous implantation of BMMSCs with HA/TCP failed to induce any up-regulation of Tregs. (**e, f**) Systemic infusion of Tregs (**e**) or BMMCs (**f**) at 2 days prior to BMMSC implantation induced a significant up-regulation of Tregs. The up-regulated Tregs gradually decreased to normal level after 9 days of infusion. (**g–i**) Different doses of Tregs were infused to C57BL6 mice. Tregs at 1×10^6 and 2×10^6 showed significantly elevated levels of Tregs than 0.1×10^6 and 0.5×10^6 groups at indicated time points (**g**). 0.1×10^6 and 0.5×10^6 Treg infusion group failed to promote bone formation in subcutaneous BMMSC implants (**h**). However, Tregs at 1×10^6 and 2×10^6 groups showed similar effect in promoting bone formation in BMMSC implants (**h**). Image J semi-quantitative analysis showed the amount of new bone formation in each group (**i**). (*$P < 0.05$, **$P < 0.01$, $n = 5$). Scale bar, 100 μm.

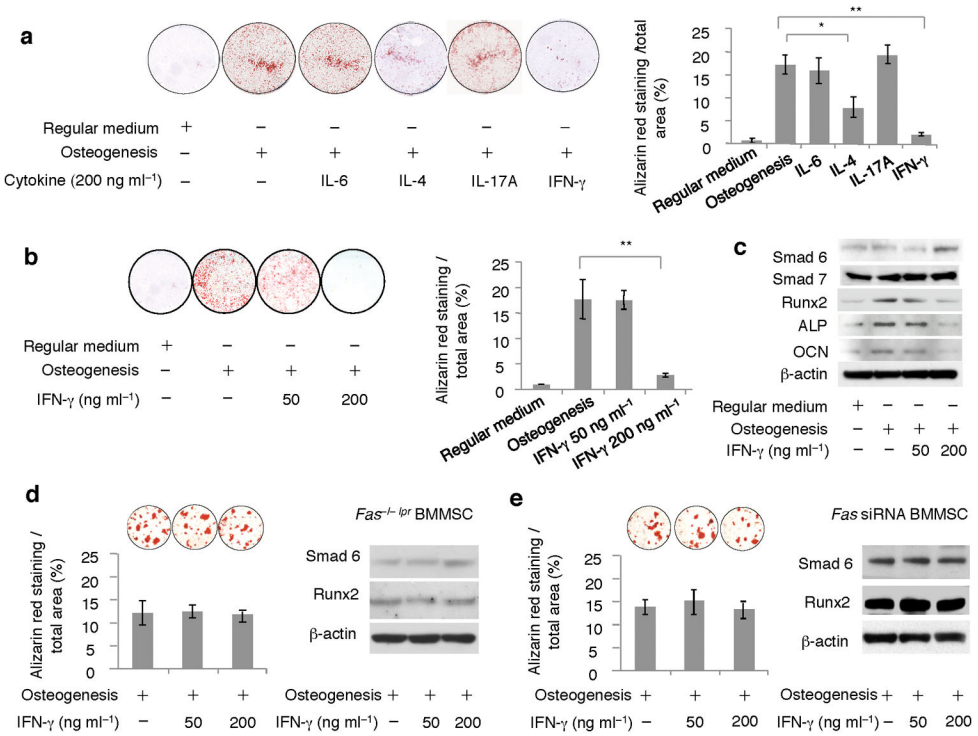

Figure 3. IFN-γ inhibited osteogenic differentiation of BMMSCs

(**a**) When BMMSCs were co-cultured with 200 ng ml^{-1} IL-4, IL-6, IL-17A, and IFN-γ in osteogenic medium for 14 days, alizarin red staining showed that IFN-γ treatment significantly inhibited mineralized nodule formation when compared to osteogenic inductive (osteogenesis), IL-4, IL-6, and IL-17A groups. IL-4 treatment reduced mineralized nodule formation. But IL-6 and IL-17A treatment had no inhibition effect on the mineralized nodule formation. (**b**) When 50 ng ml^{-1} IFN-γ was used to treat BMMSCs, there was no significant inhibitive effect on mineralized nodule formation compared to osteogenic inductive group as evidenced by alizarin red staining. However, 200 ng ml^{-1} IFN-γ treatment showed a significant reduction in mineralized nodule formation. (**c**) Western blot analysis showed that IFN-γ at 200 ng ml^{-1} elevated Smad 6 expression and inhibited expression levels of osteogenic genes Runx2, ALP and OCN, which were not observed in 50 ng ml^{-1} IFN-γ treatment group. Expression level of Smad 7 was not altered in IFN-γ-treated BMMSCs. (**d, e**) IFN-γ treatment failed to block osteogenesis and alter expression levels of Smad 6 and Runx2 in *Fas*$^{-/-}$ BMMSCs derived from *lpr* mice (**d**) and *Fas* knock down BMMSCs by siRNA (**e**) as assessed by alizarin red staining and Western blot analysis, respectively. (*P < 0.05, **P < 0.01, n = 5).

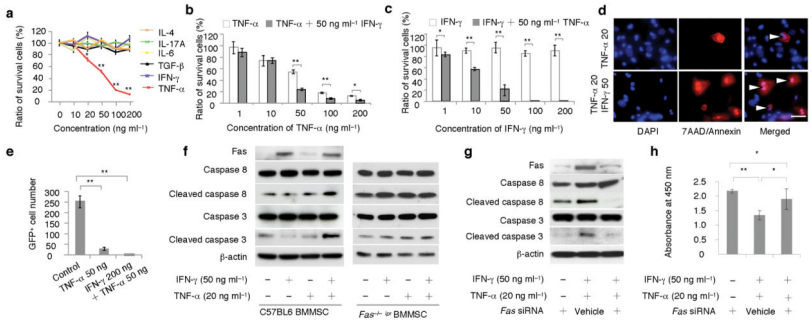

Figure 4. IFN-γ synergistically enhanced TNF-α-induced BMMSC apoptosis *via* Fas apoptotic pathway

(a) IL-4, IL-6, IL-17A, TGF-β1, IFN-γ, and TNF-α at various concentrations (1, 10, 20, 50, 100, 200 ng ml^{-1}) were cultured with BMMSCs for three days. Only TNF-α induced a dose-dependent cell death and other cytokines showed no effect on BMMSC death as evidenced by toluidine blue staining. (**b**) TNF-α (50 ng ml^{-1} to 200 ng ml^{-1}) induced BMMSC apoptosis was synergistically enhanced by IFN-γ treatment (50 ng ml^{-1}) as assessed by toluidine blue staining. (**c**) IFN-γ (1–200 ng ml^{-1}) was not able to induce BMMSC apoptosis. With adding TNF-α (50 ng ml^{-1}), a dose dependent BMMSC death was observed from 1 to 50 ng ml^{-1} IFN-γ groups. When IFN-γ concentration reached higher than 100 ng ml^{-1}, there was no any BMMSC survived in the cultures. (**d**) Representative images showed that IFN-γ (50 ng ml^{-1}) accelerated TNF-α (20 ng ml^{-1}) induced BMMSC apoptosis (triangles, TNF-α 20 ng ml^{-1} and IFN-γ 50 ng ml^{-1}) as evidenced by 7AAD/Annexin staining when compared to TNF-α treatment group (TNF-α 20). (**e**) When BMMSCs (4 × 10^{6}) were subcutaneously implanted into nude mice with matrigel containing TNF-α (50 ng ml^{-1}) showed a marked reduction in the numbers of survived BMMSCs compared to untreated control group at 30 days post implantation. Moreover, combined treatment of TNF-α (50 ng ml^{-1}) and IFN-γ (200 ng ml^{-1}) resulted in a completely no BMMSC survived at 30 days post implantation. **(f)** IFN-γ (50 ng ml^{-1}) treatment induced up-regulated expression of Fas in wild type BMMSCs along with no activation of caspase 3 and caspase 8. TNF-α (20 ng ml^{-1}) treatment showed slightly increase in Fas expression and caspase 3 activity as evidenced by Western blot analysis. When co-stimulated with IFN-γ and TNF-α, expression levels of Fas, cleaved caspase 8 and 3 were significantly elevated when compared to TNF-α treatment group. Interestingly, BMMSCs derived from *Fas*$^{-/-}$ *lpr* mice showed no response to IFN-γ and TNF-α treatment in terms of expression of cleaved caspase 8 and 3. (**g, h**) When Fas expression was partially blocked by siRNA, Western blot analysis showed that expression levels of cleaved caspase 8 and 3 were reduced in IFN-γ/TNF-α-treated group (**g**), along with a significantly reduction of survived cells (**h**). (*P < 0.05, **P < 0.01, n = 5). Scale bar, 50 μm.

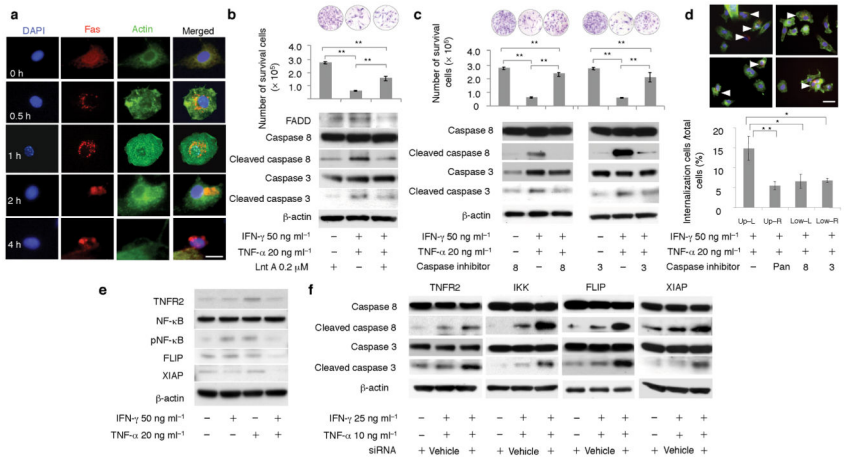

Figure 5. IFN-γ synergistically enhanced TNF-α-induced BMMSC apoptosis *via* inhibition of TNFR2/NFκB pathway and Fas internalization

(a) Fluorescent immunocytostaining showed that Fas and actin were localized on BMMSC surface and in cytoplasm, respectively (0 h). IFN-γ (50 ng ml^{-1}) and TNF-α (20 ng ml^{-1}) treatment resulted in Fas internalization and clustering in BMMSCs as shown in indicated time points (0.5–4 hours). A marked BMMSC apoptosis was observed at 2–4 hours IFN-γ/TNF-α treatment. (**b**) When endocytosis inhibitor Lnt A was used to treat BMMSC for 3 hours, IFN-γ/TNF-α-induced cell death and activation of cleaved caspase 8 and 3 were significantly reduced as assessed by toluidine blue staining and Western blot analysis. (**c**) Caspase 8 inhibitor treatment reduced levels of cleaved caspase 8 and 3 in IFN-γ/TNF-α-treated BMMSCs, which was associated with rescuing IFN-γ/TNF-α-induced cell death as shown by toluidine blue staining. Caspase 3 inhibitor was also capable of rescuing IFN-γ/TNF-α-induced BMMSC death with partially inhibition of cleaved caspase 3 and no inhibitive effect on cleaved caspase 8. (**d**) Blockage of caspase activities using pan caspase inhibitor (upper-right), caspase 8 inhibitor (lower-left), or caspase 3 inhibitor (lower-right) reduced number of Fas internalization when compared to control group (upper-left). (**e**) Western blot analysis showed that IFN-γ/TNF-α treatment resulted in a decreased expression of TNFR2, phosphorylated NFκB (pNFκB), FLIP, and XIAP when compare to TNF-α-treated BMMSCs. (**f**) Inhibition of TNFR2, IKK, FLIP, and XIAP using siRNA led to up-regulation of cleaved caspase 8 and 3 in IFN-γ (25 ng ml^{-1})/TNF-α (10 ng ml^{-1}) treated BMMSCs. (*$P < 0.05$, **$P < 0.01$, $n = 5$). Scale bar, 20 μm (**a**), 50 μm (**d**).

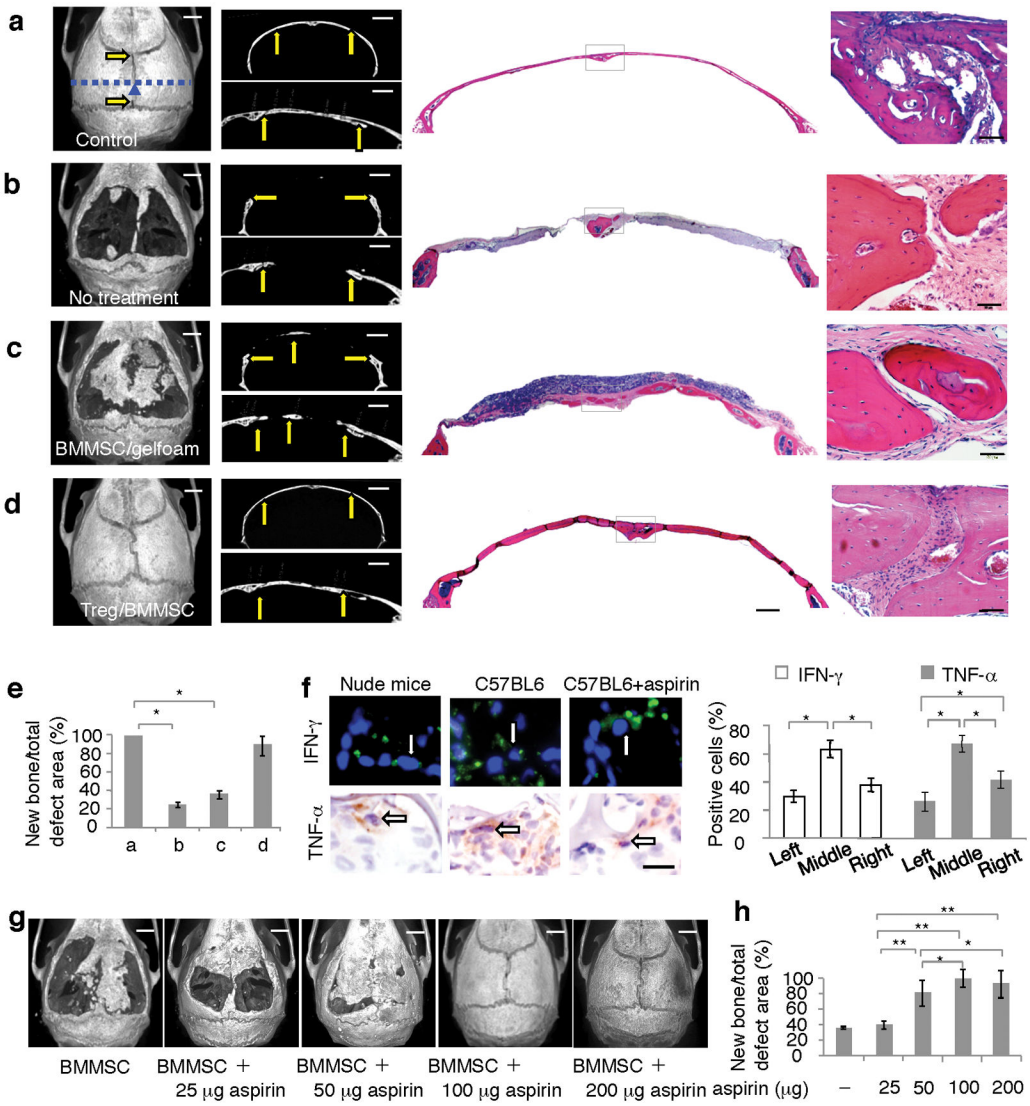

Figure 6. Treg infusion and aspirin treatment improved BMMSC-mediated bone formation for repairing calvarial bone defects in C57BL6 mice

(**a**) Normal calvarial bone showed general microCT image of sutures (arrows) and intact bone structure (left panel), coronal microCT image (upper-middle panel) and sagittal microCT image (lower-middle panel). H&E staining showed coronal calvarial bone (right panel) and suture area (far right panel). (**b**) 7 × 8 mm critical-sized calvarial bone defects were generated in C57BL6 mice, very limited amount of bone formation was identified at 12 weeks post surgery as shown by general microCT image (left panel). The calvarial defect was shown by coronal microCT image (upper-middle panel) and sagittal microCT image (lower-middle panel). H&E staining showed the coronal calvarial defect (right panel) and suture area with newly formed bone (far right panel). (**c**) With implantation of BMMSCs using gelfoam as a carrier, there was certain amount bone regeneration at 12 weeks post implantation, but failed to completely repair the calvarial defects (left panel). The repair area of the calvarial defect was shown by coronal microCT image (upper-middle panel) and sagittal microCT image (lower-middle panel). H&E staining showed the repaired coronal

calvarial defect (right panel) and suture area (far right panel). (**d**) Tregs were infused into the recipient mice at 2 days prior to BMMSC/gelfoam implantation, a totally repairing of the calvarial defects was observed at 12 weeks post implantation (left panel). The repair area of the calvarial defect was shown by coronal microCT image (upper-middle panel) and sagittal microCT image (lower-middle panel). H&E staining showed the repaired coronal calvarial defect (right panel) and suture area (far right panel). (**e**) MicroCT quantitative analysis showed amount of bone formation in each group. (**f**) Immunohistochemical staining showed that the numbers of IFN-γ and TNF-α positive cells were higher in BMMSC implants in C57BL6 mice in comparison to BMMSC implants in nude mice. There were significantly decreased levels of IFN-γ and TNF-α in aspirin treated group when compare to untreated control group in C57BL6 mice. (**g**) 4×10^6 BMMSCs were cultured with 50 μg ml^{-1} aspirin for 2 days and subsequently seeded into 7 × 8 mm calvarial bone defect areas using hydrogel as carrier, which contained 0, 25, 50, 100, and 200 μg aspirin. Gelfoam containing 2×10^6 BMMSCs and 100 μg aspirin was used to cover hydrogel/BMMSC complex prior to the suture. At 12 weeks post implantation, microCT analysis showed that calvarial defects were partially repaired at 25–50 μg aspirin groups and completely repaired at 100 and 200 μg aspirin groups. (**h**) Image J semi-quantitative analysis showed relative amount of bone formation in calvarial defect area. (**P* < 0.01, *n* = 5; G: galform; B: bone). Scale bar, 1,000 μm (left, upper-left and lower-left panels of **a–d, g**), 500 μm (left panels of **a–d**), 100 μm (far left panels of **a–d**), 50 μm (**f**).